Tech Science Press

Improved Thermal Efficiency of Salinity Gradient Solar Pond by Suppressing Surface Evaporation Using an Air Layer

Asaad H. Sayer[1] and Hameed B. Mahood[2,*]

[1]Department of Chemistry, College of Science, University of Thi-Qar, Thi-Qar, Iraq
[2]Department of Chemical and Process Engineering, Faculty of Engineering and Physical Sciences, University of Surrey, Guildford, UK
*Corresponding Author: Hameed B. Mahood. Email: hbmahood@yahoo.com

Abstract: Salinity gradient solar ponds (SGSPs) provide a tremendous way to collect and store solar radiation as thermal energy, and can help meet the critical need for sustainable ways of producing fresh water. However, surface evaporation results in the loss of both water and heat. This study therefore theoretically investigates the effect on temperatures within an SGSP when its surface is covered with a layer of air encased in a nylon bag. An earlier SGSP model was slightly modified to add the air layer and to estimate the temperature distributions of the upper layer or the upper convective zone (UCZ) and the bottom layer or lower convective zone (LCZ). The results for a year-long period showed that adding the air cover increased the LCZ temperature to a maximum of 94°C in July, with a total average increase of about 9% over the uncovered pond. In the UCZ, temperatures showed an average increase of approximately 45%, reaching a maximum of 34°C. The temperature of the air layer was meanwhile found to be close to the ambient temperature and behaved identically. These findings invite future experimental and theoretical investigations into the use of air layers to prevent surface evaporation, thereby enhancing the efficiency of SGSPs as a source of clean energy.

Keywords: Salinity gradient solar pond; modeling; air layer; thermal performance

Nomenclature

A_{air}:	Surface area of the air bag containing the air (m^2)
A_{LCZ}:	Surface area of the LCZ (m^2)
A_{UCZ}:	Surface area of the UCZ (m^2)
a:	constant
b:	constant
c_{pair}:	Air heat capacity (J/kg K)
c_{pLCZ}:	Heat capacity of water in the LCZ (J/kg K)
c_{pUCZ}:	Heat capacity of water in the UCZ (J/kg K)
h_c:	Convective heat transfer coefficient from the UCZ to the air layer (W/m^2 K)
h_{cair}:	Convective heat transfer coefficient from the air bag to the air (W/m^2 K)
h_1:	Heat transfer coefficient between the NCZ and the UCZ (W/m^2 K)

h_2:   Heat transfer coefficient between the LCZ and the NCZ (W/m^2 K)
h_3:   Convective heat transfer coefficient at the boundary between the storage zone and the surface at the bottom of the pond
h_4:   Convective heat transfer coefficient at the surface of the ground water sink
k_g: Thermal conductivity of the ground under the pond (W/mK)
K_w: Thermal conductivity of water (W/m K)
Q_{bottom}:   Heat loss to the ground through the base of the pond (W/m^2)
Q_{cond}:   Conductive heat loss from the surface of the UCZ to the air layer (W/m^2)
$Q_{conv(air)}$:   Heat loss by convection from the surface of the air layer (W/m^2)
Q_I: Incident solar radiation (W/m^2)
Q_{load}:   Heat extraction from the LCZ (W/m^2)
Q_{RLCZ}:   Solar radiation entering and stored in the LCZ (W/m^2)
Q_{Ri}:   Solar radiation entering the UCZ (W/m^2)
Q_{Ro}:   Solar radiation exiting the UCZ (W/m^2)
Q_{RUCZ}:   Solar radiation absorbed in the UCZ (W/m^2)
Q_{rad}:   Radiation heat loss from the surface of the air layer to the atmosphere (W/m^2)
Q_{stored}:   Heat stored in the LCZ (kJ)
Q_{uconv}:   Heat loss by convection from the surface of the UCZ to the air layer (W/m^2)
Q_{ue}:   Heat loss from the surface of the UCZ by evaporation (W/m^2)
Q_w: Walls heat loss of the pond (W/m^2)
T_a: Ambient temperature (°C)
T_{air}:   Temperature of the air inside the nylon bag (°C)
T_k: Sky temperature (K)
T_{LCZ}:   Temperature of water in the LCZ (°C)
T_{UCZ}:   Temperature of water in the UCZ (°C)
ΔT: Temperature difference (°C)
t: Time (month)
U_t: Overall heat transfer coefficient (W/m^2 K)
v: Wind speed (m/s)
X_{air}:   Thickness of the air layer (nylon bag) covering the UCZ (m)
X_{LCZ}:   Depth of the LCZ (m)
X_{NCZ}:   Depth of the NCZ (m)
X_{UCZ}:   Depth of the UCZ (m)
x_g: Distance of the water table from the bottom of the pond (m)
η: Efficiency
ϵ: Emissivity of water
σ: Stefan-Boltzmann constant (5.673 × 10^{-8} W/m^2 K^4)
ρ_{air}:   Air density (kg/m^3)
ρ_{LCZ}:   Density of water in the LCZ (kg/m^3)
ρ_{UCZ}:   Density of water in the UCZ (kg/m^3)

1 Introduction

The significant increase in global demand for energy has led scientists and companies to seek sustainable and clean sources of renewable energy, especially by harnessing solar power. Solar ponds are an inexpensive technique to capture and efficiently store incident solar radiation, and offer a viable solution to the quest for reduced dependence on fossil fuel. Salinity gradient solar ponds (SGSPs) have been widely constructed and have been the focus of considerable investigation [1–6]. It is a simple and inexpensive technology that can

provide thermal energy throughout the year—even in winter—particularly for industries and uses that require only a temperature below 100°C to function [7–14].

Of the various industrial applications that can be coupled to SGSPs, water desalination is one of the highest-energy consumption processes—but is also among the most significant [15]. There is a critical need for affordable, clean and sustainable energy resources that are suitable for supplying heat for the production of fresh water. In the climates in which solar energy applications are deployed, solar ponds can potentially provide enough heat to drive different desalination processes, and can do so efficiently and cost-effectively [16–21]. Many studies have recommended further research on the development of thermal storage and particularly the use of renewable [22,23]. It is therefore vital that SGSPs are fully understood in order to maximise their potential use. This includes the need for further investigation of ways to reduce surface evaporation, which is the main focus of the present study.

An SGSP is a body of water designed for the collecting and storing incident solar radiation. Commonly SGSP build with a depth of between 2 and 5 m, with vertical variations in salt concentrations to suppress natural convection [24]. It has three distinct zones: the upper convective zone (UCZ), non-convective zone (NCZ) and lower convective zone (LCZ). The UCZ or surface zone is commonly made from local fresh water or low salinity brine; it is mainly homogenous, and makes the pond more stable. Below it, the NCZ has a vertical salinity gradient (concentration gradient) within the layer; in other words, the salt concentration increases from the top to the bottom of the zone. In SGSP technology, natural convection currents are suppressed by the salinity gradient in the NCZ, ensuring that heat loss from the LCZ to the UCZ and finally to the atmosphere occur only by the mechanism of conduction. The LCZ, at the bottom of the pond, has the highest salinity or salt concentration. The layer (LCZ) is designed to collect and store the absorbed solar radiation.

Evaporation is a vital difficulty and affects the performance and viability of SGSPs. Reducing or even eliminating this surface evaporation potentially decreases the amount of water required to maintain the pond, as well as decreasing heat loss. Sayer et al. [25] theoretically investigated the amount of heat lost from the top surface of the UCZ of an SGSP, concluding that heat was lost mainly through evaporation from the surface. The collected results demonstrated that suppressing evaporation from the UCZ of the pond might potentially increase the temperature in both the UCZ and LCZ. Sayer et al. [26] investigated the addition of a very thin layer of paraffin liquid to the surface of an SGSP to eliminate evaporation. The layer successfully eliminated evaporation; however, it was also observed that, whereas the addition of paraffin layer had no effect on the salinity gradient of the NCZ throughout the study period, there was a significant change in the temperature profile to be approximately uniform throughout the water body of the pond after about 50 days. Dust had also accumulated on top of the paraffin layer. Adding paraffin to the surface could therefore negatively affect the penetration of solar radiation to the bottom of the pond, and could also have negative environmental consequences; consequently it was considered that more environmentally friendly alternatives were worthy of investigation. Ruskowitz et al. [27] experimentally observed that suppressing surface evaporation from an SGSP led to an apparent improvement in the temperature of the LCZ. It was also concluded that there was a drop in the amount of heat lost to the atmosphere; simultaneously, temperatures of the UCZ and the top layers of the NCZ increased significantly. Many other studies have also confirmed that evaporation has a significant and negative effect on SGSP performance [1–3]. Arid areas with noticeable or high evaporation levels would lose more heat and water to the atmosphere than other regions. The elimination of this loss presents probably the most difficult challenge for researchers to address. The prevention of evaporation from the surface of SGSP would also remarkably enable SGSPs to be utilised in places with water shortages, where the water needed for the replacement of the UCZ is reduced.

The suppression of evaporation from an SGSP in laboratory conditions was also investigated by Ruskowitz et al. [27]. Three types of transparent plastic covers were used. The results showed that

evaporation decreased by 47%, while the temperature of the LCZ increased by 26%. Another useful experimental study was carried out by Assari et al. [6] over a three-month period in summer in the Iranian city of Dezful: evaporation decreased significantly when a plastic cover was used, and the LCZ temperature was enhanced.

The present study theoretically investigates the elimination of evaporation from the surface of an SGSP by covering it with a layer of air, and studies the temperature changes in the air cover and the upper and lower convective zones. It introduces theoretical data in which this method has suppressed evaporation to a high degree with no negative influence on the environment. Practically, the new approach using the air layer is easier than using a thin covering of liquid, which presents difficulties in essential maintenance tasks such as washing and replenishing the UCZ. An air cover also reduces the effect of wind on the UCZ, which cannot be achieved with the liquid cover. Furthermore, air is transparent, environmentally friendly and has very low density, and the air cover (bag) can easily float on water. The study was based on the model developed by Sayer et al. [25], which had previously been verified by comparison with experimental data, and were modified to include the air layer.

2 Mathematical Formulation

This paper used a modified version of the model developed by Sayer et al. [25] to predict variations in the temperatures of the different zones within a solar pond as a result of introducing an air layer floating on the top of the UCZ, as shown in Fig. 1.
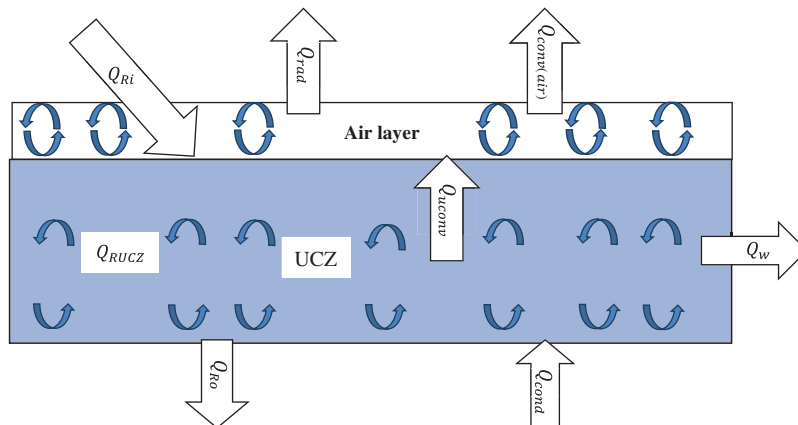

Figure 1: Schematic of UCZ with air layer on top

2.1 Air Layer

The air layer covering the UCZ was considered to comprise a nylon bag filled with air of 0.1 m thickness, as represented schematically in Fig. 2. For simplification, several assumptions were made in developing the overall energy equation of this layer, as follows: (i) it was assumed that no solar radiation has accumulated in the air layer; (ii) conduction heat transfer through the nylon was neglected; (iii) it was assumed that the cover suppressed 80% of surface evaporation; Ruskowitz et al. [27] found that covering around 80% of the surface area of the pond was the efficient method to achieve the maximum LCZ temperature; and there is no change in the physical properties with the temperature change; and (iv) it was assumed that the walls of the pond were well insulated (i.e., there was no heat loss through the walls).
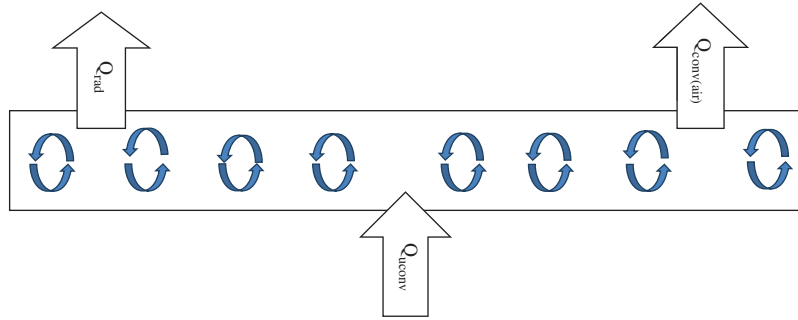
Figure 2: Schematic of the air layer

The heat balance equation of the air layer would be expressed as below:

$$\rho_{air}c_{pair}A_{air}X_{air}\frac{dT_{air}}{dt} = [Q_{uconv} - Q_{conv(air)} - Q_{rad}] \tag{1}$$

The symbols Q_{uconv} and $Q_{conv(air)}$ represent respectively the heat loss by convection from the surface of the UCZ to the air layer, and that from the surface of the air layer to the atmosphere. They are given as:

$$Q_{uconv} = h_c A_{UCZ}[T_{UCZ} - T_{air}] \tag{2}$$

$$Q_{conv(air)} = h_{cair}A_{air}[T_{air} - T_a] \tag{3}$$

$$h_{cair} = 5.7 + 3.8 \text{ v} \tag{4}$$

where h_c and h_{cair} are respectively the convective heat transfer coefficients between the UCZ and the air layer ($h_c = 5.7$, because the effect of wind speed is neglected), and between the air layer and surrounding air (atmosphere) [28]. Q_{rad} represents the radiation heat loss to the atmosphere, and is given as:

$$Q_{rad} = \sigma\epsilon A_{air}\left(T_{air}^4 - T_k^4\right) \tag{5}$$

In Eq. (5) σ represents the Stefan-Boltzmann constant and ϵ is the water emissivity (0.83) [15]. The symbol T_k represents the temperature of the sky and it is computed as [25]:

$$T_k = 0.0552T_{air}^{1.5} \tag{6}$$

2.2 Upper Layer (UCZ)

Fig. 3 shows the UCZ of the pond. As it had been supposed that 80% of evaporation was being prevented, only 20% of evaporation heat loss was considered. It was considered that this level of evaporation could occur through spaces among the air bags.

The energy conservation equation of the UCZ can be given as:

$$\rho_{UCZ}c_{pUCZ}A_{UCZ}X_{UCZ}\frac{dT_{UCZ}}{dt} = Q_{RUCZ} + Q_{cond} - Q_{uconv} - Q_{ue} - Q_w \tag{7}$$

The walls of the ponds were considered to be well insulated (no heat loss, $Q_w = 0$). Eq. (7) is therefore can be expressed as:

$$\rho_{UCZ}c_{pUCZ}A_{UCZ}X_{UCZ}\frac{dT_{UCZ}}{dt} = Q_{RUCZ} + Q_{cond} - Q_{uconv} - Q_{ue} \tag{8}$$

In Eq. (8), Q_{RUCZ} is the absorbed solar radiation in the UCZ. It can be calculated as:

$$Q_{RUCZ} = Q_{Ri} - Q_{Ro} \tag{9}$$

where Q_{Ri} represents solar radiation that enters the UCZ and Q_{Ro} is the solar radiation that leaves it.

The incident radiation can also be computed or recorded from data available in climatological stations from the location of a pond. In this study, NASA climatological data was used [29] to calculate Q_{RUCZ} using a simple expression was used as [8]:

$$h_x = Q_{Ri}(a - b\ln x) \tag{10}$$

where a = 0.36, b = 0.08, and x is the depth of the water layer (in metres); it was claimed that the formula was valid for water depths from 0.01 and 10 m [8]. The symbol h_x is the quantity of solar radiation in any depth of water. That means Eq. (10) can be written as:

$$h_x = Q_{Ri}(0.36 - 0.08\ln x) \tag{11}$$

In the present study, Eq. (11) was used to calculate the solar radiation absorbed in the water body of the pond. Hence Eq. (9) becomes:

$$Q_{RUCZ} = Q_{Ri}(1 - 0.36 + 0.08\ln X_u) \tag{12}$$

Conduction heat transfer from the LCZ to the UCZ is calculated as below [26]:

$$Q_{cond} = U_t A_{UCZ}[T_{LCZ} - T_{UCZ}] \tag{13}$$

where T_{LCZ} and T_{UCZ} represent respectively temperatures of the lower convective zone (LCZ) and the upper convective zone (UCZ). The symbol U_t is the overall heat transfer coefficient; it is calculated as [25]:

$$U_t = \frac{1}{\frac{1}{h_1} + \frac{X_{NCZ}}{k_w} + \frac{1}{h_2}} \tag{14}$$

In Eq. (14), h_1 and h_2 are respectively the convective heat transfer coefficients between the NCZ and the UCZ, and between the LCZ and the NCZ. Values of h_1 and h_2 were given respectively as 56.58 and 48.279 W/m^2 K [7]. The symbol k_w represents the thermal conductivity of water: its value was given as 0.596 W/m K [7]. The symbol X_{NCZ} represents the depth of the NCZ.

Eq. (13) can be written as:

$$Q_{cond} = \frac{A_{UCZ}[T_{LCZ} - T_{UCZ}]}{\frac{1}{h_1} + \frac{X_{NCZ}}{K_w} + \frac{1}{h_2}} \tag{15}$$

The evaporation heat loss was calculated using the equation of [18]:

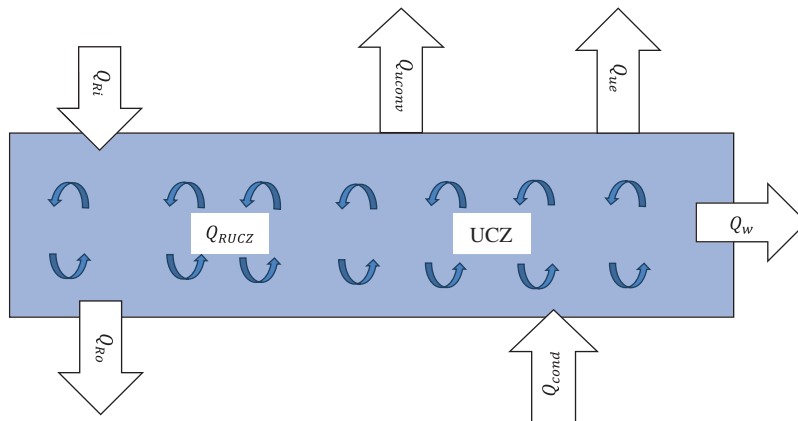$$Q_{ue} = \left\{ \frac{\lambda h_c [p_{UCZ} - p_a]}{[(1.6C_s p_{atm})]} \right\} A_{UCZ} \tag{16}$$

Figure 3: Schematic of the upper convective zone

where λ is the latent heat of vaporization; and Cs is given in kJ/kg and represents the humid heat capacity of air. The definitions and values of the variables of Eq. (16) were given in Sayer et al. [25].

2.3 Lower Convective Zone

Fig. 4 illustrates schematically the storage zone or the LCZ of the pond.

It was supposed that there was no load (no heat extraction) from the LCZ and consequently the zone was storing solar radiation as thermal energy. It was also considered that there was heat loss from the top and from the bottom (to the ground), but no heat loss to the atmosphere from the walls of the considered pond. The heat balance equation of the LCZ can be described as:
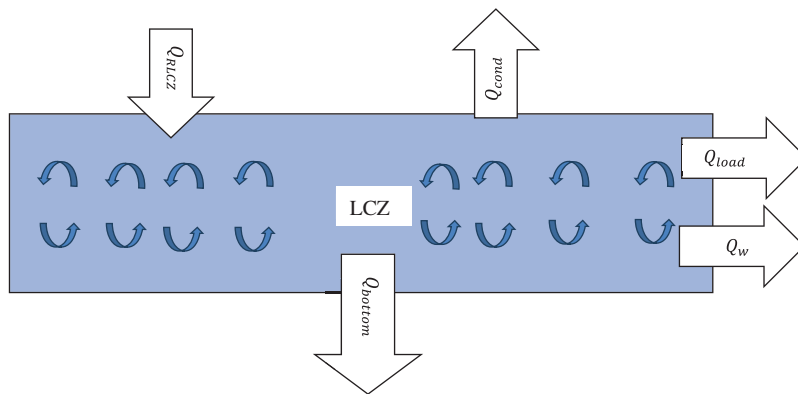

Figure 4: Schematic of the LCZ

$$\rho_{LCZ} c_{pLCZ} A_{LCZ} X_{LCZ} \frac{dT_{LCZ}}{dt} = Q_{RLCZ} - Q_{cond} - Q_{bottom} - Q_{load} - Q_w \tag{17}$$

Considering the assumptions of no heat extraction (no load, $Q_{load} = 0$) and no heat loss through the walls of the pond ($Q_w = 0$), Eq. (17) converts to:

$$\rho_{LCZ} c_{pLCZ} A_{LCZ} X_{LCZ} \frac{dT_{LCZ}}{dt} = Q_{RLCZ} - Q_{cond} - Q_{bottom} \tag{18}$$

To calculate Q_{bottom}, the following equation is used:

$$Q_{bottom} = U_{ground}A_b(T_{LCZ} - T_g)$$ (19)

where U_{ground} represents the overall heat transfer coefficient to the bottom (the base of the pond); this is taken [25] as:

$$U_{ground} = \frac{1}{\frac{1}{h_3} + \frac{x_g}{k_g} + \frac{1}{h_4}}$$ (20)

In Eq. (19), A_b represents the area of the base of the pond which is in contact with the ground; h_3 is the convective heat transfer coefficient at the barrier between the storage zone and the surface at the bottom of the pond; and h_4 is the convective heat transfer coefficient at the surface of the ground water sink. The values of h_3 and h_4 are 78.12 and 185.8 W/m^2 K respectively [7]. Eq. (19) is written as:

$$Q_{bottom} = \frac{A_b(T_{LCZ} - T_g)}{\frac{1}{h_3} + \frac{x_g}{k_g} + \frac{1}{h_4}}$$ (21)

The solar radiation absorbed in the LCZ (Q_{RLCZ}) has been computed by the use of Eq. (10) as:

$$Q_{RLCZ} = Q_{Ri}(0.36 - 0.08\ln(X_{UCZ} + X_{NCZ}))$$ (22)

3 Results and Discussion

Eqs. (1), (8) and (18) have been solved using MATLAB. The initial values of the unknown temperatures T_{air}, T_{UCZ} and T_{LCZ} were given to solve these equations. The values of the constants (ρ_{UCZ}, ρ_{LCZ}, c_{pUCZ}, c_{pLCZ}, h_1, h_2, h_3, h_4, k_w, and T_g) were taken from [25]. The values of x_g and k_g are dependent on the nature of the soil under the base of the pond; their values were given in [30]. The pond was considered to be in Nasiriya City, Iraq, and was considered to have dimensions of $1 \times 1 \times 1.5$ m with layer depths of 0.2, 0.8 and 0.5 m for the UCZ, NCZ and LCZ respectively.

3.1 Temperature of the Lower Convective Zone

The temperature profile along a year of the LCZ is shown in Fig. 5. This figure clearly shows a continuous increase in the LCZ temperature between January (during the winter) and July (during the summer). To demonstrate the influence of the incident solar radiation on the LCZ temperature, its profile was plotted against time, as also illustrated in Fig. 5.

It is apparent that the behaviour of the LCZ temperature is similar to that of the incident solar radiation. The solar radiation increases from winter towards summer, reaching its maximum level in June, followed by a continuous decrease towards its minimum level in December. Fig. 5 also shows that the maximum temperature of the LCZ was in July around 94°C, a month after the peak in solar radiation, which might be due to the accumulation of thermal heat in the LCZ, shifting the maximum value from June to July. After this point, the LCZ temperature shows a regular decrease towards its minimum level in December. Sayer et al. [26] concluded that incident solar radiation significantly affected evaporation from the surface of the SGSP: their results showed that evaporation increased with the increase of solar radiation. It was also concluded that further increases in solar radiation led to further increases in the LCZ temperature. This finding has been confirmed by many other researchers [31,32]. However, Sayer et al. [26] also found that evaporation was influenced significantly (negatively) by the increase in ambient temperature, which
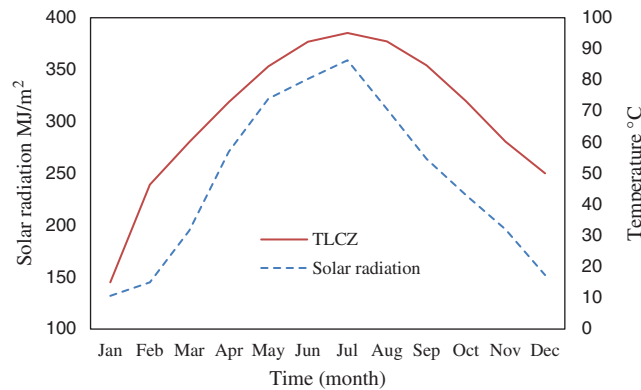
Figure 5: Profiles of the incident solar radiation in Nasiriya City, Iraq, for one year; and of the LCZ temperature in a pond covered with an air layer considered to be in Nasiriya City. The pond had a surface area of 1 m² and depths of 0.2, 0.8, and 0.5 m for the UCZ, NCZ and LCZ respectively

increased as incident solar radiation increased. Their results also demonstrated that the temperatures of the UCZ and LCZ followed the behaviour of the incident solar radiation and ambient temperature.

A comparison between LCZ temperatures in the covered and uncovered (conventional) ponds is shown in Fig. 6. It is clear from Fig. 6 that the LCZ temperature in the covered pond was mostly higher than in the conventional pond during all 12 months of the study year. The difference was about 6°C from March to December, and the maximum LCZ temperature in the covered pond reached 94°C compared with around 88°C in the conventional one. The results showed an average increase in LCZ temperature of about 9%. The LCZ temperatures in both ponds were shown to behave identically during the study period: both of them steadily increased, attained their maximum value in July, and then steadily decreased to reach their minimum values in December.
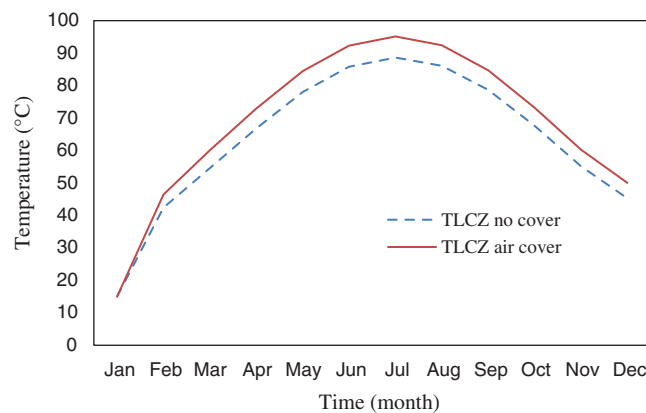

Figure 6: Comparison between LCZ temperatures in covered and uncovered pond; the pond is considered to be in Nasiriya City, Iraq. The pond had a surface area of 1 m² and depths of 0.2, 0.8, and 0.5 m for the UCZ, NCZ and LCZ respectively

3.2 Temperature of the Upper Convective Zone

The UCZ temperature distributions for both the covered and conventional ponds are shown in Fig. 7. It can be seen clearly from Fig. 7 that the addition of the air cover had a positive influence on the temperature of the UCZ. Temperature of the layer (UCZ) in the covered pond increased over time to reach a maximum value
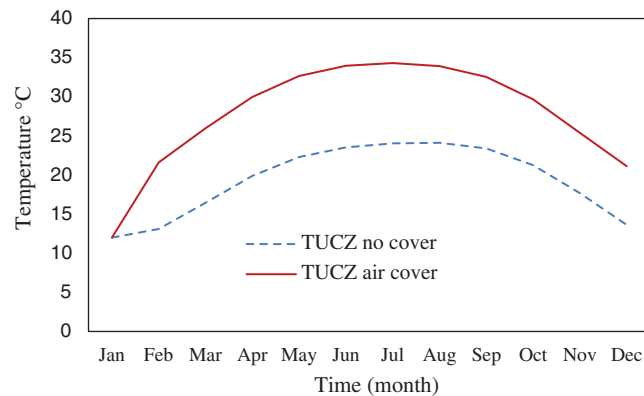
Figure 7: UCZ temperature profiles of the covered and uncovered ponds; the pond is considered to be in Nasiriya City, Iraq. It had a surface area of 1 m^2 and depths of 0.5, 0.8 and 0.2 m for the LCZ, NCZ and UCZ respectively

in July of more than 10°C above that of the uncovered pond, which achieved its maximum in in June. The UCZ temperature in the covered pond increased by approximately 47% over the levels achieved in the conventional pond, reaching around 34°C between May and September. It has previously been suggested that the UCZ absorbs about 45% of the incident solar radiation [9], energy which is lost again to the environment, mainly by evaporation. Suppressing or diminishing surface evaporation means that the absorbed radiation is captured as thermal heat in the UCZ, increasing its temperature and potentially converting it to a new thermal storage zone. The results of the present investigation agree with the conclusions of many previous studies [26,27,31].

3.3 Temperature of the Air Cover

The temperature of the air cover is presented in Fig. 8, which also shows the temperature of the UCZ and the ambient temperature. It is evident from Fig. 8 that throughout the one-year period of the study, the temperature of the air cover was close to the ambient temperature. There is a gap between the UCZ temperature on the one hand, and the temperatures of both the air cover and the ambient temperature on the other.
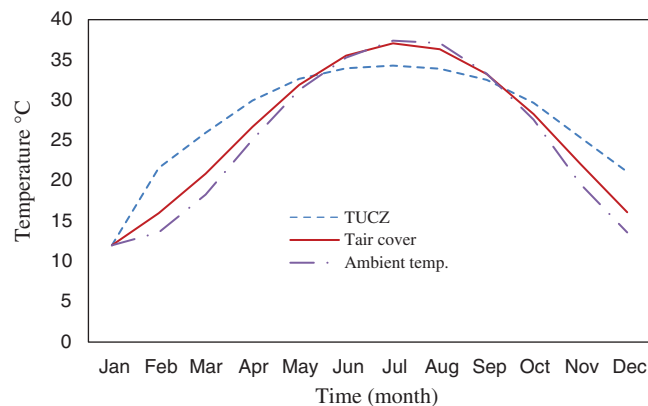

Figure 8: Temperature profiles of the air cover, ambient temperature and UCZ of the pond; the pond is considered to be in Nasiriya City, Iraq. It had a surface area of 1 m^2 and depths of 0.5, 0.8 and 0.2 m for the LCZ, NCZ and UCZ respectively

It can be seen from Fig. 8 that for months June to September, the ambient temperature is higher than the UCZ temperature. Consequently heat could be transferred from the atmosphere to the UCZ by the mechanism of convection. Same behavior was observed by Sayer et al. [25] and Huanmin et al. [33].

Finally, to evaluate the efficiency of the two solar ponds (covered and uncovered), the stored energy as heat in their LCZ is calculated and compared using the following equation:

$$Q_{stored} = \rho_{LCZ} c_{pLCZ} A_{LCZ} X_{LCZ} \Delta T_{LCZ} \tag{23}$$

where ΔT represents the temperature difference in the LCZ, and ($\rho_{LCZ} A_{LCZ} X_{LCZ}$) water mass of the LCZ.

Fig. 9 illustrates the variation of the stored energy in the LCZ of the two ponds with time when there was no heat extraction from the two ponds. It is obvious from Fig. 9 that heat stored in the LCZ of the two ponds is following the behaviour of the incident solar radiation and hence the temperature profile of the LCZ (see Fig. 6). In both ponds, energy stored increases gradually with the time progress, reaches its maximum value at June (at summer), and then regularly decreases and come to its minimum value at November (at winter). This could be simply justified according to the principle of energy balance as manifested in Eq. (23). Where with the same mass of the working fluid (water) and initial temperature of the two ponds, the effective parameter that can determine the amount of energy stored in the LCZ is the final temperature of the LCZ. Therefore, it is apparent from Fig. 9 that the energy stored in the covered pond is higher than that of the uncovered pond (conventional) during the period of the study due to the clear difference of the time dependent LCZ temperature as pointed out by Fig. 6. However, the maximum difference of the stored energy in the LCZ between the covered and uncovered pond was about 9.6% at June (summer).
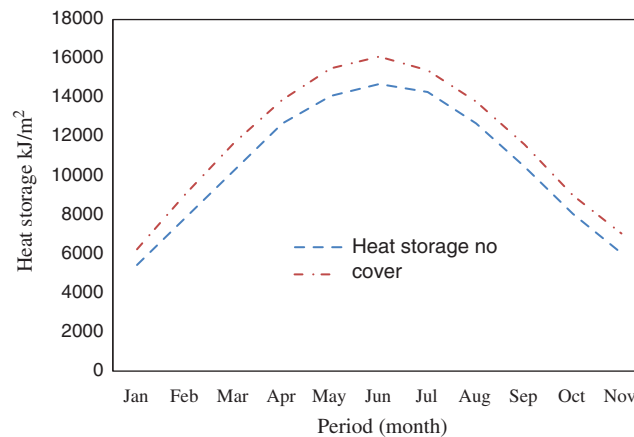

Figure 9: Variation of heat storage of covered and uncovered pond with time. The pond is considered to be in Nasiriya City, Iraq. It had a surface area of 1 m^2 and depths of 0.5, 0.8 and 0.2 m for the LCZ, NCZ and UCZ respectively

Additionally, efficiency of the two ponds can be calculated according to the following equation:

$$\eta = \frac{Q_{stored}}{Q_I} \tag{24}$$

where Q_I is the incident solar radiation on the top surface of the covered and uncovered ponds.

In according to Eq. (24), the efficiency of the covered pond was found to be higher than the uncovered pond by about 4% (as a maximum). However, the efficiency was calculated when no heat extraction was considered. In this case, the temperature of the LCZ increased to reach the highest value where a balance

between heat gain and heat loss is sustained. Consequently, the difference in efficiency of the two ponds is convergence. On the other hand, when the heat is continuously extracted from the pond, the temperature is decreased with time and due to the large temperature difference, it will absorb more solar radiation so that to substitute the removed heat. In this case the efficiency of the pond would be meaningful.

4 Conclusion

This study has aimed to compute the temperatures of the LCZ, UCZ and air layer of a covered salinity gradient solar pond. It was considered that the pond was covered with an air cover with a thickness of 0.1 m to eliminate surface evaporation. The pond was considered to be in Nasiriya City, Iraq, with a surface area of 1 m^2 and a total depth of 1.5 m, made up of layers that were respectively 0.5, 0.8 and 0.2 m deep for the LCZ, NCZ and UCZ, respectively. Temperatures of the UCZ and LCZ in the covered pond were seen to increase by 47% and 9% respectively over those in the uncovered pond. It was also observed that the temperature patterns of the covered pond behaved identically to those of the conventional pond. In addition, the stored energy as heat in the LCZ and efficiency of the covered pond was found to be higher than the uncovered pond by about 9.6% and 4% (as a maximum) respectively. The findings of this investigation invite more studies in this field.

Conflicts of Interest: The authors declare that they have no conflicts of interest to report regarding the present study.

References

1. Akbarzadeh, A., Ahmadi, G. (1979). Under ground thermal storage in the operation of solar ponds. *Energy, 4(6),* 1119–1125. DOI 10.1016/0360-5442(79)90102-6.

2. Date, A., Akbarzadeh, A. (2013). Salinity gradient solar ponds. In: Napoleon, E., Akbarzadeh, A. (eds), *Energy Sciences and Engineering Applications.* CRC Press. E. Book. Chapter 7, pp. 195–218, Taylor & Francis Group.

3. Alagao, F. B. (1996). Simulation of the transient behavior of a closed-cycle salt-gradient solar pond. *Solar Energy, 56(3),* 245–260. DOI 10.1016/0038-092X(95)00073-Z.

4. Dehghan, A. A., Movahedi, A., Mazidi, M. (2013). Experimental investigation of energy and energy performance of square and circular solar ponds. *Solar Energy, 97,* 273–284. DOI 10.1016/j.solener.2013.08.013.

5. Antipova, E., Boer, D., Cabeza, L. F., Gosalbez, G. G., Jimenez, L. (2013). Multi-objective design of reverse osmosis plants integrated with solar Rankine cycles and thermal energy storage. *Applied Energy, 102,* 1137–1147. DOI 10.1016/j.apenergy.2012.06.038.

6. Assari, M. R., Tabrizi, H. B., Nejad, A. K., Parvar, M. (2015). Experimental investigation of heat absorption of different solar pond shapes covered with glazing plastic. *Solar Energy, 122,* 569–578. DOI 10.1016/j. solener.2015.09.013.

7. Bansal, P. K., Kaushik, N. D. (1981). Salt gradient stabilized solar pond collector. *Energy Conversion and Management, 21(1),* 81–95. DOI 10.1016/0196-8904(81)90010-8.

8. Bryant, H. C., Colbeck, I. (1977). A solar pond for London? *Solar Energy, 19(3),* 321–322. DOI 10.1016/0038-092X(77)90079-2.

9. Akbarzadeh, A., Andrews, J., Golding, P. (2005). Solar pond technologies: a review and future directions. *Advances in Solar Energy, 16,* 233–294.

10. El Mansouri, A., Hasnaoui, M., Amahmid, A., Dahani, Y. (2018). Transient theoretical model for the assessment of three heat exchanger designs in a large-scale salt gradient solar pond: energy and exergy analysis. *Energy Conversion and Management, 167,* 45–62. DOI 10.1016/j.enconman.2018.04.087.

11. Amini, H., Wang, L., Shahbazi, A. (2016). Effects of harvesting cell density, medium depth and environmental factors on biomass and lipid productivities of *Chlorella vulgaris* grown in swine wastewater. *Chemical Engineering Science, 152,* 403–412. DOI 10.1016/j.ces.2016.06.025.

12. Ghaffour, N., Lattemann, S., Missimer, T., Kim, C. N., Sinha, S. et al. (2014). Renewable energy-driven innovative energy-efficient desalination technologies. *Applied Energy, 136,* 1155–1165. DOI 10.1016/j.apenergy.2014.03.033.

13. Karakilcik, M., Kiymac, K., Dincer, I. (2006). Experimental and theoretical temperature distributions in a solar pond. *International Journal of Heat and Mass Transfer, 49(5–6),* 825–835. DOI 10.1016/j.ijheatmasstransfer.2005.09.026.

14. Gude, V. G. (2015). Energy storage for desalination processes powered by renewable energy and waste heat sources. *Applied Energy, 137,* 877–898. DOI 10.1016/j.apenergy.2014.06.061.

15. Hull, J. R., Nielsen, C. E., Golding, P. (1988). *Salinity gradient solar ponds*. Florida: CRC Press.

16. Kasaeian, A., Shakiba, S., Yan, W. M. (2018). Novel achievements in the development of solar ponds: a review. *Solar Energy, 174,* 189–206. DOI 10.1016/j.solener.2018.09.010.

17. Jaefarzadeh, M. R. (2004). Thermal behavior of a small salinity-gradient solar pond with wall shading effect. *Solar Energy, 77(3),* 281–290. DOI 10.1016/j.solener.2004.05.013.

18. Kishore, V. V. N., Joshi, V. (1984). A practical collector efficiency equation for nonconvecting solar ponds. *Solar Energy, 33(5),* 391–395. DOI 10.1016/0038-092X(84)90190-7.

19. Liu, X., Caoa, G., Shena, S., Gua, M., Li, C. (2013). The research on thermal and economic performance of solar desalination system with salinity-gradient solar pond. *Desalination and Water Treatment, 51(19–21),* 3735–3742. DOI 10.1080/19443994.2013.795021.

20. Kumar, A., Singh, K., Verma, S., Das, R. (2018). Inverse prediction and optimization analysis of a solar pond powering a thermoelectric generator. *Solar Energy, 169,* 658–672. DOI 10.1016/j.solener.2018.05.035.

21. Leblanc, J., Akbarzadeh, A., Andrews, J., Lu, H., Golding, P. (2011). Heat extraction methods from salinity-gradient solar ponds and introduction of a novel system of heat extraction for improved efficiency. *Solar Energy, 85(12),* 3103–3142. DOI 10.1016/j.solener.2010.06.005.

22. Krishnasamy, K., Renganathan, M. (2017). Effect of lower convective zone thickness and swirl flow on the performance of a salinity gradient solar pond. *Chemical Engineering Transactions, 62,* 283–288.

23. Mahfoudh, I., Safi, M. J. (2018). Experiment study of the effect of salt on the stability of solar ponds. *Environmental Progress and Sustainable Energy (AICHE), 38(2),* 699–705.

24. Salata, F., Coppi, M. (2014). A first approach study on the desalination of sea water using heat transformers powered by solar ponds. *Applied Energy, 136,* 611–618. DOI 10.1016/j.apenergy.2014.09.079.

25. Sayer, A. H., Al-Hussaini, H., Campbell, A. N. (2016). New theoretical modelling of heat transfer in solar ponds. *Solar Energy, 125,* 207–218. DOI 10.1016/j.solener.2015.12.015.

26. Sayer, A. H., Al-Hussaini, H., Campbell, A. N. (2017). Experimental analysis of the temperature and concentration profiles in a salinity gradient solar pond with, and without a liquid cover to suppress evaporation. *Solar Energy, 155,* 1354–1365. DOI 10.1016/j.solener.2017.08.002.

27. Ruskowitz, J. A., Suarez, F., Tyler, S. W., Childress, A. E. (2014). Evaporation suppression and solar energy collection in a salt-gradient solar pond. *Solar Energy, 99,* 36–46. DOI 10.1016/j.solener.2013.10.035.

28. McAdams, W. H. (1954). *Heat transmission*. Third Edition. Tokyo, Japan: McGraw-Hill, Kogakusha.

29. NASA (2019). Surface meteorology and solar energy, a renewable energy resource. https://eosweb.larc.nasa.gov.

30. Sayer, A. H., Al-Hussaini, H., Campbell, A. N. (2018). New comprehensive investigation on the feasibility of the gel solar pond, and a comparison with the salinity gradient solar pond. *Applied Thermal Engineering, 130,* 672–683. DOI 10.1016/j.applthermaleng.2017.11.056.

31. Suarez, F., Ruskowitz, J. A., Tyler, S. W., Childress, A. E. (2015). Renewable water: direct contact membrane distillation coupled with solar ponds. *Applied Energy, 158,* 532–539. DOI 10.1016/j.apenergy.2015.08.110.

32. Torkmahalleh, M. A., Askari, M., Gorjinezhad, S., Eroglu, D., Obaidullah, M. et al. (2017). Key factors impacting performance of a salinity gradient solar pond exposed to Mediterranean climate. *Solar Energy, 142,* 321–329. DOI 10.1016/j.solener.2016.12.037.

33. Lu, H., John, C. W., Andrew, H. P. (2001). Desalination coupled with salinity-gradient solar ponds. *Desalination, 136(1–3),* 13–23. DOI 10.1016/S0011-9164(01)00160-6.